

Optimization on Pole Pitch of Magnetic Wheels and Thickness of Metal Plate for Floating and Propulsion System using Permanent Magnets

T. Saiki¹, K. Ino¹, M. Inada¹

¹Faculty of Engineering Science, Kansai University, 3-3-35 Yamate, Suita, Osaka. 564-8680, Japan

E-mail: tsaiki@kansai-u.ac.jp

Abstract

A magnetic-levitation system using a rotating permanent magnet has been developed. Pole pitch of the magnetic wheels and thickness of the metal plates required for levitation were investigated by experiments and computational calculation.

To determine the optimum conditions, the levitation force generated by using motors with different torque and rotation speed was measured. These measurements clarified differences in the generated levitation force due to the different rotational speed and torque. Parameters such as skin depth, magnetic density, and eddy-current distribution density, ratio of drag force to levitation force, and levitation force per driving power were numerically calculated from the magnetic field created by the rotating permanent magnet and effective frequency.

General important conclusion obtained from the calculation was that the magnetic wheels should be designed to be large and the pole pitch of the magnets was to be wide, and the levitation force per driving power will be improved in proportion to a root function of the pole pitch between the magnets. If the size of the magnetic wheel increased, the ratio of the lateral drag force per the levitation force became significantly small at low rotational speed. A motor with a large torque and peak output property at low rotational speed for magnetic wheels is most suitable for driving large magnetic wheels to obtain large levitation force.

Using large magnetic wheel in the experiment showed that the levitation force per driving power increased than that case of using small magnetic wheel.

Keyword—Magnetic floating, Magnetic wheel, Permanent magnet, Eddy current.

I. INTRODUCTION

Many railway and mobile systems using magnetic levitation force have been proposed [1], and many magnetic levitation systems that use the attractive force of a magnetic field have also been proposed. Some of them use a superconducting magnet, which needs to be cooled to an extremely low temperature by using a cryogenic fluid such as liquid nitrogen. A coil is required on the wall and maintenance is also required. EDS using a coil has been proposed, but it is difficult for the coil to generate the strong magnetic field required for levitation.

Researches on a magnetic levitation and propulsion system using a rotating permanent magnet that does not require a superconducting magnet have been conducted. Such systems can obtain a large levitation force and acceleration force [2]-[5]. In a levitation system using magnetic wheels, not only the levitation force but also the propulsive force to move forward can be obtained by using the electromagnetic force generated by the magnet rotating at a high speed. As the shape of the magnetic wheel, a type [2] in which a magnet is placed on the outside of the wheel, a surface in contact with a metal surface, and a thin plate-shaped substrate such as an axial flux type motor [6] or a generator [7] exist. Thus, two types of methods in which magnets are placed and rotated at high speed have been researched.

A plan for a hyperloop is under consideration in the United States [8]. A future transportation system that can move at high speed in a vacuum was proposed. As one of the plans, an EDS (Electromagnetic Suspension System), which moves a fixed magnet at high speed and floats, has been proposed and studied [9]. In that transportation system, magnets are fixed to a moving body that can obtain a levitation force by generating an eddy current when accelerated to a certain speed by some method [9]. In the system, a device generating a stronger magnetic force based on the Halbach array has also been proposed [9, 10].

Until now, researches on the theoretical calculation of the levitation force and propulsion force produced by the rotating permanent magnets and the generation of the levitation force using a copper plate or an aluminum plate have been conducted, and the characteristics in the low-speed rotation region have been clarified [3-5]. However, property of the levitation force in the high-speed rotation region at 20000 rpm and the reduction of the thickness of the metal plate used have not been studied and discussed.

We studied reduction mechanism of driving power for magnetic wheels and reduction of metal plate thickness. The distribution of magnetic field, current density, and levitation force are calculated numerically.

Experiments and computer simulations were conducted to be cleared them in this time. And, we report the results of those studies.

II. THEORY

The levitation principle of a magnetic levitation propulsion system using a rotating permanent magnet is explained below using Fig. 1. Some numerical calculations related to eddy currents and levitation forces generated on metal surfaces have been performed in the past [9], [11]-[17]. It is assumed that there is a rotating permanent magnet and the magnetic field of the permanent magnet moving in space is close to the metal plate. When a permanent magnet is moved close to a metal plate, a loop-shaped eddy current with temporal change is generated on the copper plate according to Lenz's law. The eddy current creates a new magnetic field. When the magnetic wheels rotate at a low speed, that is, when the resistance in the conductor is sufficiently larger than the reactance, the effect of the Arago's rotation on the conductor plate changes to be remarkable. No levitation force is generated, and the metal plate is dragged in the same direction as the magnet movement.

At this time, the phase difference between the eddy current and the magnet magnetic field is almost 0 with respect to the magnet magnetic field. When the magnetic wheel rotates at a high speed, the reactance component of the eddy current on the metal plate becomes dominant, and the magnetic force due to the eddy current acts to cancel the magnetic field generated the magnet. Thus, a repulsive force is generated. Changing the point of view, at the same time, a new magnetic field component perpendicular to the eddy current on the metal surface and the magnetic field of the magnet and parallel to the metal surface is generated. A Lorentz force $J \times B$ is generated by the magnetic field B and the large eddy current J , and a repulsive force is generated to push down the metal plate.

Here, using the 2-D calculation model of magnetic levitation using a magnet that moves at high speed described in the paper [9], the magnetic field created by the magnet on the copper plate is assumed to be a sine wave. The magnetic field in the metal plate given by Maxwell-Ampere and Maxwell-Faraday laws and Gauss's law for magnetics were solved.

The reasons that we use a 2D model here are 1) The problem is simplified, and 2) To find the first-order solution and major property by changing many parameters. We think that high-precision ones should be obtained by quadratic calculation.

Here, the 2-D calculation model is shown Fig. 2. The magnetic field in the depth direction in the copper plate, and the newly generated secondary magnetic field and current parallel to the copper plate were calculated. Also, the Lorentz force, which is the force that pushes down the metal plate that works due to this magnetic field and current, was calculated.

The equation of the distribution of the magnetic field traveling in the time-varying- x direction on the copper plate is shown next.

$$B_g(t) = B_g \cdot \sin\left(\pi \frac{x}{\tau} + \omega_s t\right)$$

$$\omega_s = \frac{v_s}{r} = 2\pi f \quad (1)$$

Here, v_s is the moving speed of the magnet. r is the distance from the center of the magnetic wheel to the center of Nd magnet. Thus, r is the radius. B_g is the amplitude of the magnetic field in the z direction created by the magnetic field of the magnet on the metal surface. τ is the pole pitch interval of the magnets. The magnitude of the newly generated secondary magnetic field is given by the following formula when there are magnetic fields in the x and z directions. The effective frequency with considering the number of the magnet poles is expressed by

$$f = \frac{p}{2} \cdot \frac{N}{60} \quad (4)$$

where N is the rotation speed of the magnet and p is the number of magnetic poles. For example, because two repeating eight NSs are paired, a sine magnetic wave passes four times on the same metal plate.

$$B_2(t) = B_g \cdot \exp\left(-\frac{z}{\delta_s}\right) \cdot \begin{pmatrix} -\frac{\sqrt{2}\tau}{\delta_s\pi} \cos\left(\pi\frac{x}{\tau} + \omega_s t - \frac{z}{\delta_s} + \frac{\pi}{4}\right) \\ 0 \\ \sin\left(\pi\frac{x}{\tau} + \omega_s t - \frac{z}{\delta_s}\right) \end{pmatrix} \quad (2)$$

The skin depth of each newly generated magnetic field into the metal plate is calculated by the following equation, which is an index of the penetration depth of the electromagnetic wave.

This is an equation that normally defines the range in which a high-frequency current flows through the copper wire.

$$\delta_s = \sqrt{\frac{2\rho}{\omega_s \cdot \mu_0}} \quad (3)$$

Here, ρ is the electrical resistivity of the metal plate, and ω represents the angular frequency of the alternating magnetic fields generated by the alternately arranged permanent magnets.

Although μ_0 is conventionally the magnetic permeability in vacuum, it is assumed here that it is the magnetic permeability of the conductor.

The newly generated secondary current density is expressed by the following equation.

$$j_{2y} = -\frac{B_g^2}{\mu_0} \cdot \frac{2\tau}{\delta_s^2 \pi} \cdot \exp\left(-\frac{z}{\delta_s}\right) \cdot \sin\left(\pi \frac{x}{\tau} + \omega_s t - \frac{z}{\delta_s}\right). \quad (6)$$

The current exists only in the y direction. The equation of the Lorentz force pushing down the metal plate generated by the current and the secondary magnetic field is expressed by

$$F_L = J_{2y} \times B_{2x} . \quad (7)$$

The force density generated from the secondary magnetic field generated in the x direction and the current is expressed by

$$F_L = -\frac{B_g^2}{\mu_0} \cdot \exp\left(-\frac{2z}{\delta_s}\right) \cdot \frac{2\tau}{\delta_s^2 \pi} \cdot \sin\left(\pi \frac{x}{\tau} + \omega_s t - \frac{z}{\delta_s}\right) \cdot \frac{\sqrt{2}\tau}{\delta_s \pi} \cos\left(\pi \frac{x}{\tau} + \omega_s t - \frac{z}{\delta_s} + \frac{\pi}{4}\right). \quad (8)$$

This is the levitation force which exists only in the z direction. The integral of this in the x direction and the thickness z direction gives the following equation. It gives the levitation force generated per 1 m in the y direction.

$$F_{Ltot} = \int_0^L \int_0^d f_L \cdot dzdx \quad (9)$$

The relational equation between the output power of the motor and the torque T is

$$T = \frac{P}{2\pi \frac{N}{60}} . \quad (11)$$

The levitation force generated is calculated by the next equation [4]

$$F_L = k_0 \sigma \cdot P.$$

$$\sigma = \frac{1}{C_d v_s} = \frac{F_z}{F_x v_s} = \frac{\tau}{v_s \pi \delta_s}.$$

(12)

Here, F_L/P is the levitation force per required power to rotating magnetic wheel.

$C_d = F_x/F_z$ is the drag force ratio. σ is a levitation force per unit required power. However, it can be regarded as constant at the low-speed rotational speed where the levitation force rises firstly from the experimental results. This constant k_0 should also change depending on the structure of the magnetic wheel and on the driving method. Fujii et al. have reported many characteristics of driving power and driving torque related to the generation of levitation force by rotating permanent magnets when copper plates and aluminum plates are used [3-5]. As a result, it was shown that the levitation force saturates at higher rotation speeds. The cause of saturation is not the skin effect due to the bias of the eddy current at the surface of the conductor due to levitation. The saturation of the levitation force depends on the saturation of the generated magnetic field in the horizontal direction.

When the rotation speed is low, the torque increases proportionally to the rotation speed as a synchronous motor, but when the rotation speed of the magnetic wheel rises to 2000 rpm (magnet speed 10 m / s), it reaches a peak and the above phase shift is large. Therefore, the drive torque for rotating the magnetic wheels is reduced. When comparing the saturation of the levitation force between the copper plate and the aluminum plate, the saturation property tends to be stronger in the copper plate with lower resistivity [3-5].

III. EXPERIMENT AND CALCULATION METHOD

A method for measuring the levitation force of the magnetic wheel is described here. The levitation force measuring device of the magnetic wheel used in this work is shown in Fig. 2. In this work, three types of motors were used to drive the magnetic wheels. The rotation devices used were 1) an large electric brushless motor (FSD, FCS5055-8T, KV550, KK HOBBY, Japan), 2) a low-speed rotary brushless motor (A2212 / 13T, 1000kV), and 3) a high-speed rotary brushless motor (A2212 / 6T, 2000kV), that uses ESC drive for drones. The high-speed rotary brushless motor was also used to obtain the property of the levitating force at high-speed rotation. The brushless motors were firmly fixed to the work base.

The rotation speed of the brushless motor was controlled by sending a PWM signal for control to the ESC from the servo tester. The structure of the magnetic wheel used is shown in Fig. 3. The magnetic wheels were made of non-magnetic aluminum, and we used two types, a small one with a diameter of 4.5 cm and a large one with a diameter of 9 cm. For the small magnetic wheels, Nd magnets (residual magnetic flux density 0.32 T) with a diameter of 8 mm and a thickness of 3 mm were used. The magnets were arrayed in 8 poles at a uniform angle, and the N and S poles were arrayed alternately. For the large wheels, Nd magnets (residual magnetic flux density 0.2T) with a diameter of 15 mm and a thickness of 6 mm were used. By stacking the thickness of the magnets, it was possible to change the thickness from 3 mm to 6 mm.

At this time, the residual magnetic flux density of the Nd magnet was 0.35 T in the stack of two magnets. In this case as well, the magnets were arrayed at equal angles with 8 poles, and the N and S poles were arrayed alternately. A magnetic wheel was connected to the end of a drill or a brushless motor and was rotated close to an aluminum plate or copper plate. When the magnetic wheel rotates, a force that pushes down the aluminum plate or copper plate works. The weight scale was placed upside down and the pushing force (levitation force) was measured. A non-contact digital tachometer (SE300, SANWA, Japan) using a laser was used to measure the rotation speed of the magnetic wheels, and a reflection seal was attached to the motor to receive the reflection signal of the laser light and measure the rotation speed. The pushing force was measured using a lightweight scales (1) AXB300 01, AS ONE, Japan, 2) UDS-500N, YAMATO, Japan). two DC constant-voltage power supply (PS20-20A, TEXIO, Japan) and DC constant-voltage power supply (30V 266A MAX, PAT30-266T, KIKUSUI, JAPAN) was used to drive the motor.

It has been considered so that the drive current of the motor had sufficient margin. The output voltage of the power supply was set to be 12 V when using small magnetic wheel. Also, the output voltage of the power supply was set to be 24 V when using large magnetic wheel. The output voltages were equivalent to that of three or six Li-ion batteries in series. The gap between the magnetic wheel and the metal plate was fixed. The motors were used, and the experiment was conducted by connecting magnetic wheels to the above-mentioned two types of low-speed type and high-speed type. The force was applied to push down the magnetic wheel maximally and the maximum pushing force was measured. It is clearly hard to measure the drive torque directly due to the structure of the experimental device. Here, the torque was calculated by using eq. (11).

Next, the method of computer simulation of magnetic flux density and current density is shown. The distribution of the magnetic field generated secondarily in the z direction and the x direction was calculated by using eq. (2). The x-direction distribution of the generated current density was calculated by using eq. (6). The x-direction distribution of the generated levitation force density was calculated by using the eq. (8). The total repulsive force generated in the metal plate was calculated by using eq. (9). Eq. (3) was used to calculate the skin depth.

The used parameters in these experiments are shown in Tabel.1.

Tabel.1 Parameters

Size of magnetic wheels	
Small	Diameter:4.5cm, r=1.5cm Thickness of Nd magnet: 3mm
Large	Diameter:9.0cm, r=3.0 cm Thickness of Nd magnet: 6mm
Resistivity (Cu)	1.68×10^{-8} [Ω m] 2.0×10^{-8} [Ω m] @60°C
Resistivity (Al)	2.65×10^{-8} [Ω m]
Output voltage of power supply	
Small Brushless motor	12V
Large Brushless motor	24V
Thickness of Cu plate	0.1-0.9cm
Thickness of Al plate	0.1-0.9cm

IV. RESULTS

Measured levitation force using large magnetic wheel and Cu plate is shown in Fig.5. The experiment was conducted when the thickness of the copper plate was chosen to be 9 mm. The copper plate were equipped by stacking three plates with a thickness of 3 mm. When a copper plate is used, it is considered that the efficiency of generating the levitation force changes depending on the magnitude of the magnetic flux density. When the gap changed to be smaller, the magnetic flux density became stronger, and the levitation force increased. At 3500 rpm, the levitation force was saturated. After that, the levitation force gradually decreases with rotational speed. The reason will be that the efficiency of the motor has decreased. The rotational speed when the levitation force was saturated was 3500 rpm. F_L / P calculated by using the output power of the motor was 1.3 (N / W), and it was improved for the small motor. When the Gap was 3 mm, the levitation force decreased. This seems to be an increase in resistivity of Cu due to the generated heat.

Driving torque to rotating magnetic wheel is shown in Fig.6. It has been cleared that the levitation force strongly depends on output property of the used motor. The driving torque decayed linearly and monotonically for the rotational speed.

F_L / P is shown in Fig.7. Here, F_L / P was obtained as the levitation force divide by total electrical input power into the motor. On the other hand, the F_L / P remained constant at low

rotational speed. This switching also depends on the output power characteristics of the motor. Here, k_0 is set to 1.6 for calculation of theoretical F_L / P .

Measured levitation force using small magnetic wheel and Cu plate is shown in Fig.8. It was found that the rotation speed at which the levitation force is the same as the theoretical value.

It was found that the torque required for driving was insufficient when the high-speed rotation motor was used. A low-speed type and high-speed type brushless motors were used in order to confirm the levitation force and torque in the high-rotation-speed range. A motor that realizes a low-speed type with no load of 10000 rpm and a high-speed type of 20000 rpm was used in the experiment. The maximum levitation force was measured by pressing the magnetic wheels rotated at high speed against the metal plate keeping the ESC control PWM signal constant. The magnetic wheel with a diameter of 4.5 cm was used. At this time, the drive output and drive torque were calculated assuming that the maximum efficiency of the motor was 80%. Torque required to rotating magnetic wheel is shown in Fig.9. It was found that the torque was small when a high-speed rotary brushless motor was used. It has been shown that it can operate in a different mode than when using a low speed brushless motor. F_L / P as a function of the rotation speed is shown in Fig.10. F_L / P was almost constant for all the rotational speed for using each motor. ESC standby power was ignored at this time. It turned out that there are different states to generate the same torque. That is, it was clarified that there is an operation mode in which the rotation speed is high and the torque is small even though the same levitation force is generated. The levitation force is generated exponentially for the rotation speed of 5000–17000 rpm. Good controllability of levitation force will be obtained when using a high-speed type brushless motor. When a low-speed brushless motor was used, the optimum torque was obtained at 4000 rpm, and the torque at that time reached its maximum peak. The maximum rotation speed with no load was 12000 rpm. In the case of the high-speed rotary motor, unlike the case of the low-speed rotary motor, 18000 rpm was the optimum, and the torque peaked. Input power and output power were also maximized at that time. The rotation speed with no load was 24000 rpm. At that time, the torque was halved.

The property of the levitation force with respect to the thickness of the copper plate is described as shown in Fig. 11. Thus, the experiment was conducted to confirm how the levitation force was generated when the thickness of the metal plate was actually changed and the copper plate was used. In this case, the load was low. The experiment was conducted where the thickness of the copper plate set to 0.5 mm, 1 mm, 3,6,9 mm. The input voltage of the power supply was fixed at 12 V and current data was obtained. A small type and high-speed rotation type brushless motor was used for the magnetic wheels. The measured results of the levitation force for the rotation speed of the magnetic wheel are shown Fig. 11(a) and (b). At this time, the gap between

the time wheel and the metal plate was set to 2 mm. In the case of the copper plate, the rotation speed decreased to 5000–7000 rpm compared with the case of no load. When the thickness of the copper plate was 3–9 mm, the levitation force was almost constant. Below 3 mm, the levitation force decreased linearly with respect to the thickness. Although it is a load current, it was constant even when the thickness became small.

The pulse width of the input PWM signal was increased and the rotation speed at no load was increased to 20200 rpm. When rotated on a metal plate, the rotation speed of the motor decreased to 12000 rpm. The power is constant.

Next, the case where an aluminum plate is used is described as shown in Fig. 12. The experiment was conducted with the thickness of the aluminum plate set to 1, 3, 6, and 9 mm. The gap between the time wheel and the metal plate was set to 2 mm. The PWM signal was increased to increase the rotation speed with no load to 17000 rpm. In the case of the aluminum plate, the rotation speed degraded to 6000 rpm compared to the case of no load. When the thickness of the copper plate was 6–9 mm, the levitation force was almost constant, but when it was 6 mm or less, the levitation force could not be maintained and decreased linearly for the thickness. It was confirmed that the current, which is a load, tends to decrease as the thickness increases. Also, it was confirmed that the levitation force decreased due to the increase in thickness. The rotation speed with no load was 20200 rpm. When rotated on a metal plate, the rotation speed of the motor decreased to 12000 rpm. F_L / P as a function of thickness. (a) Cu plate, (b) Al plate was shown in Fig.13. When the thickness of the Cu plate was sufficiently thick, the F_L / P was closed to 0.045 (N / W). When the thickness of Al plate is sufficiently thick, the F_L / P was 0.03 (N / W).

Calculated skin depth as a function of pole number. (A) Using Al plate, (B) Using Cu plate is shown in Fig.14. As the pitch increases, the frequency also decreases, so the skin depth was 7000 rpm when $p = 2, 4, 8$ and 6.5, 4, 3 mm for copper and 7.5, 5, 4 mm for Al. In the case of aluminum, the resistivity is lower, so the skin depth is slightly deeper. Because the conductivity of the aluminum plate is about 1/3 lower than that of the copper plate, the thickness increased. It has been found that the thickness did not change much after 20000 rpm.

Regarding the calculation results of the magnetic field and current density distribution, in order to deepen the understanding of the results generated in the experiment, the distribution of the magnetic field and current newly generated in the metal plate were calculated. It is assumed that a small magnetic wheel model is assumed, the distance between magnets is 1.2 cm, and N and S stations are arranged alternately. The electromagnetic waves effectively generated by the magnetic field are set to travel in the $-x$ direction. The amplitude of the magnetic flux density B_g on the metal surface was set to be 0.11 (T). The maximum x value was 30 cm and the number of

spatial meshes was 150. The maximum z was 5 mm in the thickness direction, and the number of spatial meshes was 100.

In order to investigate the reason why the levitation force characteristics are saturated, each component of the magnetic field that causes the saturation was investigated.

the size of B_{2x} to B_{2z} is shown in Fig. 15. It was found that B_{2x} is smaller than B_{2z} when the rotation speed is 2000 rpm or less. The magnetic field in the x direction was saturated and increased when the rotation speed increased. It was found that the torque starts to decrease at the speed at which B_{2z} and B_{2x} are reversed when the rotational speed increased. The rotational speed at which this torque phenomenon occurs is higher in the case of using the aluminum plate. As is clear from the relationships between eqs. (1), (2), and (5), the phase difference between the secondary current and B_{2x} is $\pi / 4$ regardless of the rotation speed.

The calculated results on distribution of the magnetic flux density and the current density in the x direction at the metal surface $z = 0$. The rotation speed was 7000 rpm in Fig. 16 (a) and 17000 rpm in Fig. 16 (b). This corresponds to the case where the maximum levitation force of the brushless motor is obtained. At 17000 rpm, 7000 rpm B_{2x} increased 1.5-fold and the current density increased 5-fold.

The calculated result on the spatial distribution of the magnetic flux density and current density in the conductor in the x-z direction is shown in Fig. 17. The skin depth is 3 mm at 7000 rpm, and 2 mm at 17000 rpm, and about 60% at 17000 rpm. It was found that the phase of the secondary magnetic field and the secondary current in the z direction is delayed with respect to the traveling direction of the magnet magnetic field. It can be seen that the amplitude of B_{2z} , B_{2x} , and J_{2y} is significantly degraded over the skin thickness. The amplitude of B_x at 17000 rpm was 2.8 times that of B_z . B_{2x} and J_{2y} are in synchronous.

The calculation result of the x-direction distribution in the depth z direction of the levitation force density is shown in Fig. 16. Here, the moving speed of the magnet was assumed to be 30 m / s. The levitation force density is highest on the surface and less on the bottom layer. It became clear that it was spatially in a jump and moved over time. Also, attractive force works in some parts. A phase of 2.5 rad or more delays on the surface of the metal plate.

Calculated C_d using Cu plate as a function of pole pitch is shown in Fig. 18. The radius from the center of the magnet to the center was changed to 1.5 cm, 3, 6 cm. The rotation speed was 5000,10000 rpm. $p = 8, 4, 2$. C_d decreases when the number of poles is reduced. It was found that F_x , (related to the driving torque) decreases exponentially. Larger magnetic wheels have a wider pole pitch than smaller ones. C_d tends to be small. Thus, the driving torque is small.

Calculated C_d and F_L / P using Cu plate as a function of rotational speed is shown in Fig. 19. Here, k_0 is set to 1. Radius of 1.5, 3, 6cm was used to calculation. The pole pitch is 1.2, 2.4, 4.8 when p was 8, 4, 2.

F_L / P decreases exponentially with increasing the rotational speed regardless of the size of the magnetic wheels. When the size of magnetic wheel increases, the Cd becomes smaller from the lower rotational speed. Improvement in the F_L / P was seen at the overall rotational speed.

Calculated peak F_L / P as a function of pole pitch and comparison with experimental results using Cu plate is shown in Fig.20. It was found that the peak F_L / P is proportional to 0.75 the root of τ .

5. Discussion

For a magnetic levitation propulsion system using permanent magnets, experiments and computer simulations had been conducted to know whether the reduction of the amount of conductors used is possible with maintaining the levitation force. As a result, it had been cleared that it was possible.

In this work, two types of the motors were used, a motor with a torque peak at low-speed rotation and a motor with a torque peak at high-speed rotation. The rotational velocity of the motor is controlled by the number of windings. The paper [5] shows the characteristic that the torque is degraded exponentially and the levitation force is saturated when the radius of the magnetic wheel is 5 cm and the rotation speed is 2000 rpm. In this experiment, we succeeded in generating a peak of the levitation force in the high rotation range by utilizing the torque characteristic of the motor. It was found that the property of the levitation force for the actual rotation speed of the magnetic wheel depend on the torque property of the used motor goodly.

For using small magnetic wheel, the magnetic wheels should be used at high speeds where the motor load can be expected to reduce the drive torque. The skin effect of the eddy current becomes remarkable, and the current density varies as a function of the square of the skin thickness. Thus, the current increases in proportion to the rotation speed, so the rotation speed at which the torque saturates becomes small, and the torque reaches its peak. The saturation of the levitation force becomes remarkable. The rotation speed of the magnetic wheel should be set in the region up to 10000rpm-20000 rpm. Because the high-speed type motor has the maximum output in the high-speed region, torque for rotating the magnetic wheel cannot be sufficiently supplied in the rotation region between 10000- 20000 rpm. It becomes a characteristic that the levitation force gradually rises.

It can be seen that there is almost no change in skin thickness at 15000 rpm and 20000 rpm. When a copper plate is used, it is expected from the experimental results that the levitation force will gradually increase with increasing rotation speed and become saturated at 20000 rpm. This has the same property as an inductive motor. It was shown that even if the drive torque decreases and the rotation speed is set high, a levitation force equal to or higher than that in the low-speed

region can be obtained. Further, in this case, an advantage that the torque can be reduced. The linear characteristic of the levitation force with respect to the rotation speed becomes advantageous when controlling the rotation speed of the motor.

However, because a high eddy current density is generated on the conductor surface, the temperature of the copper plate rises and the resistivity rises when the magnetic wheel is rotated in the same place.

The difference between the experiment in this paper and the experimental conditions of other Fujii groups is that the residual magnetic flux density of Nd magnets is 1.2 T and 0.3 T.

The peak F_L / P is proportional to 0.75 times root of τ . As a result, it is considered that the F_L / P , which is the ratio of levitation force to drive power, was 0.07, which as shown in Fig. 4 is 1/4 lower than 0.3. The experimental results in this paper also show that F_L / P will be improved when the pole pitch and the size of the magnetic wheel increases. The diameter of the magnetic wheel should be large. Motor with high torque and a high maximum output is preferable because the F_L / P is high. If the pole pitch becomes to be 1 m, F_L / P will be improved by single order of magnitude.

The generated F_L also changes with the square of the magnetic flux density generated by the magnet. Thus, the coefficient should be improved.

When a copper plate is used, a large levitation force like that obtained with 9 mm cannot be obtained when the thickness is 3 mm or less. If the thickness is 3 mm or less, it is considered that the magnetic field of the magnet penetrates the metal plate and leaks downward. The calculation result on the 2D distribution of the magnetic field density at this time reveals the same condition. The 2D distribution of the magnetic flux density and the eddy current density are very similar both when the thickness is infinitely large and when it is 3 mm. By looking at the distribution in this way, it may be possible to obtain an index as to whether or not the levitation force can be maintained.

In the case of using aluminum plate, it was confirmed in the experiment that the levitation force decreased when the thickness was 6 mm or more. It is considered that the magnetic field strength distribution changes depending on the thickness. The best thickness of aluminum plate should be 6 mm. In addition, it was confirmed that the levitation force decreases when the thickness is 6 mm or more. This is because the distribution of eddy currents is different between 6 mm and 9 mm.

For the calculation result of the skin thickness, the skin thickness of the copper plate at 12000 rpm is 2.5 mm. The skin thickness of the aluminum plate at 12000 rpm was 3.5 mm. In the calculation result on the 2D magnetic field distribution, the moving direction of the magnet magnetic field is on the left side, but the distribution of the Z and X direction magnetic fields

generated secondarily is deflected to the right side in the X direction as the thickness increases, and a phase delay occurred.

Regarding propulsion of this system, we plan to obtain propulsion by tilting the magnetic wheels or using vertically rotating magnetic wheels with magnets placed horizontally.

Summery

1. The diameter of the magnetic wheel should be large. Small ones are inefficient. Motor with high torque and a high maximum output is preferable because the F_L / P is high.
2. The number of poles of magnetic wheels should be reduced as much as possible. The minimum is to use 2 poles. However, considering the reduction of vibration during rotation of the wheels, 4 poles are considered to be optimal.
3. It is necessary to use a copper plate which is thicker than the skin thickness.
4. For F_L / P , F_L / P gradually declined after keeping constant.

The power to maintain high-speed rotation is greater than the torque reduction. The same story applies to the inductor-truck-type linear EDS. The speed should be limited by the input power.

6. Conclusion

We optimized the thickness of the aluminum plate and copper plate required for a magnetic levitation propulsion system using permanent magnets. The thickness of the lower metal plate required for levitation in this magnetic levitation propulsion system was investigated.

The skin depth was calculated from the magnetic field generated by the moving magnet and the frequency of the generated effective electromagnetic wave. A levitation force measurement was conducted using motors with different characteristics to search for the optimum conditions for the rotational speed.

The magnetic wheels should be designed to be large and the pole pitch of the magnets was to be wide to obtain high levitation force, and the levitation force per driving power will be improved proportional to a root function of the pole pitch between the magnets. If the size of the magnetic wheel increased, the ratio of the levitation force and the drag force ratio became significantly small at low rotational speed. A motor with a large torque and peak output property at low rotational speed for magnetic wheels is most suitable for driving large magnetic wheels to obtain large levitation force. However, the required metal will be thick because the skin depth is thick. Using large magnetic wheel in the experiment showed that the levitation force per driving power increased than that case of using small magnetic wheel.

The authors report there are no competing interests to declare

REFERENCES

- [1] M. Iwaya, S. Ozaki, H. Tamura: “Magnetic levitation system of linear motor car Linimo, Fuji Electric journal, Vol.79. No.2, pp.123-127 (2006)
- [2] J. Bird, T.A. Lipo: “Calculating the forces created by an electrodynamic wheel using a 2-D steady-state finite-element method“, IEEE Trans. Magn., Vol. 44, No.3 , pp. 365–372(2008)
- [3] N. Fujii, K. Ogawa, T. Matsumoto: “Revolving Permanent Magnet Type Magnet Wheels”, IEE Trans. Japan, Vol. 115-D, No. 3, pp.319-326 (1995) [in Japanese]
- [4] N. Fujii, K. Ogawa, M. Chida: “Relation between Magnetic Poles and Characteristics of Revolving Permanent Magnet Type Magnet Wheel“, IEE Japan, Vol. 117-D, No. 6, pp.768-775, (1997) [in Japanese]
- [5] N. Fujii, G. Hayahsi, Y. Sakamoto, “Characteristics of Self-driven Magnet Wheel and Maglev Test Car Using the Wheels”, IEE Trans. Japan, Vol. 115-D, No. 3, pp.319-326. (1995) [in Japanese]
- [6] K.M. Rahman, N.R. Patel, T.G. Ward, J.M. Nagashima, F. Caricchi, F. Crescimbin: “Application of Direct-Drive Wheel Motor for Fuel Cell Electric and Hybrid Electric Vehicle Propulsion System”, IEEE Trans. on Industry Applications, Vol. 42, Issue: 5, pp.1185-1192 (2006)
- [7] T. Saiki, T. Matsuzaki, T. Yasuki, T. Nakaya, M. Inada: “Axial-Flux Generator Using a Sintered Iron Nano-Polycrystalline Body”, J. of Electronic Materials Vol. 50, pp. 5995-6005 (2021).
- [8] P.E. Ross : “Hyperloop: no pressure”, IEEE Spectr. , Vol.53, No.1, pp. 51–54 (2016)
- [9] M. Flankl, T. Wellerdieck , A. Tüysüz , J. W. Kolar, “Scaling laws for electrodynamic suspension in high-speedtransportation”, IET Electric Power Applications, Vol.12, No.3, pp. 357-364 (2018)
- [10] R.F. Post, D.D. Ryutov: ‘The inductrack: a simpler approach to magnetic levitation’, IEEE Trans. Appl. Supercond., Vol. 10, No.1, pp. 901–904 (2000)
- [11] R. Knowles: “Dynamic circuit and Fourier series methods for moment calculation in electrodynamic repulsive magnetic levitation systems”, IEEE Trans. Magn., Vol. 18, No.4, pp. 953–960 (1982)
- [12] W. Ko, C. Ham: “A novel approach to analyze the transient dynamics of an electrodynamic suspension maglev”, IEEE Trans. Magn., Vol.43, No.6, pp.2603–2605 (2007)
- [13] M. Carlstedt, K.W. nee Porzig, M. Ziolkowski, et al.: “Estimation of Lorentz force from dimensional analysis: similarity solutions and scaling laws“, IEEE Trans. Magn., Vol. 52, No.8, pp. 1–13 (2016)
- [14] K. Ogawa, Y. Horiuchi, N. Fujii: “Calculation of electromagnetic forces for magnet wheels”, IEEE Trans. Magn., Vol. 33, No.2, pp. 2069–2072 (1997)
- [15] J.H. Park, Y.S. Baek: ‘Design and analysis of a maglev planar transportation vehicle’, IEEE Trans. Magn., Vol. 44, No.7, pp. 1830–1836 (2008)

- [16] D. Rodger , T. Karguler, P.J. Leonard: “A formulation for 3D moving conductor eddy current problems”, IEEE Trans. Magn., Vol. 25, No.5, pp.4147–4149 (1989)
- [17] D. Yonetsu, K. Tanaka, T. Hara, “Examination of Buoyancy-Reduction Effect in Induction-Heating Cookers by Using 3D Finite Element Method”, IEE Trans. Japan, Vol. 130-D, No. 5, pp.590-598. (2010)

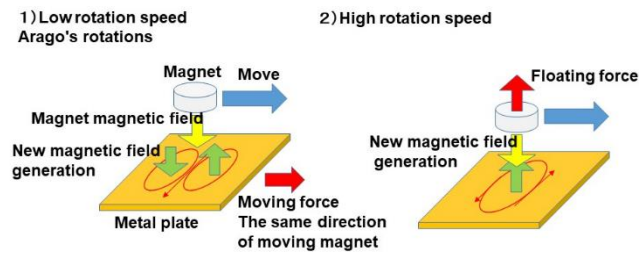


Fig.1 Principle of magnetic floating.

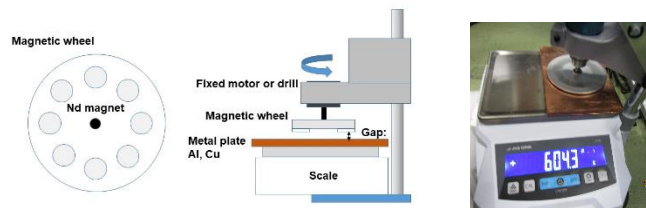


Fig.2 Instrument for measuring floating force of magnetic wheel.

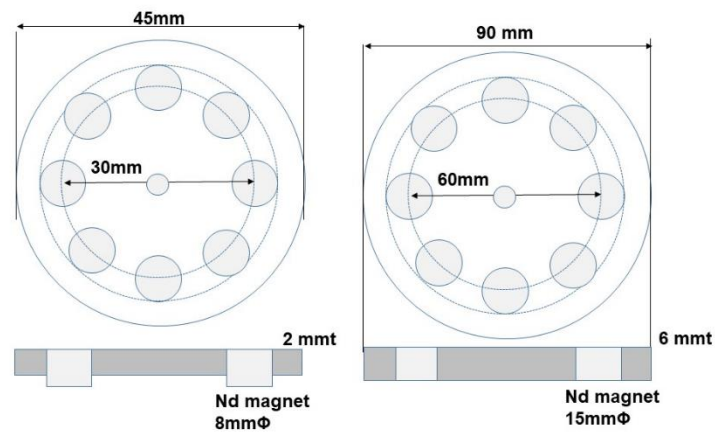


Fig.3 Structure of magnetic wheels. Left: small magnetic wheel, Right: large magnetic wheel

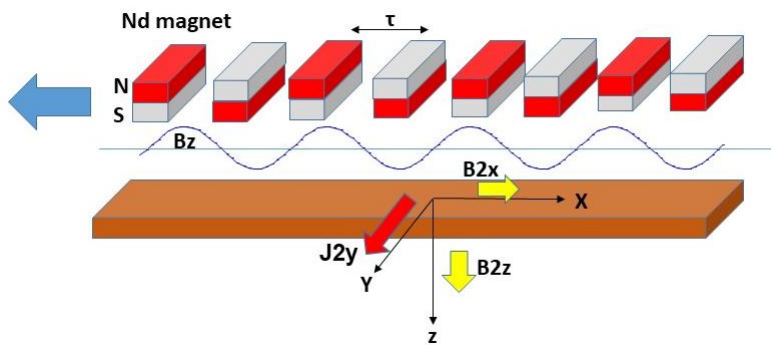


Fig.4. 2-D calculation model.

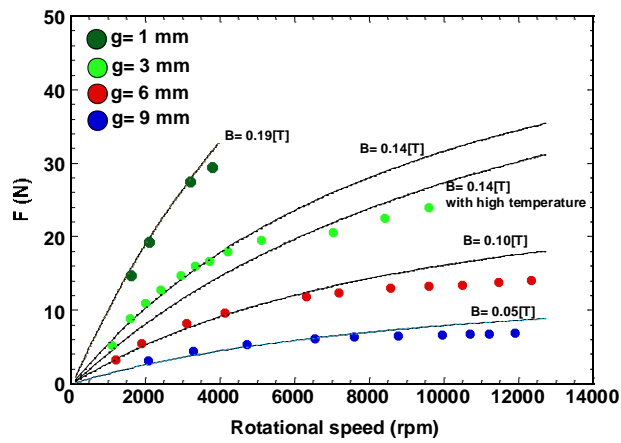


Fig.5 Measured levitation force using large magnetic wheel and Cu plate.

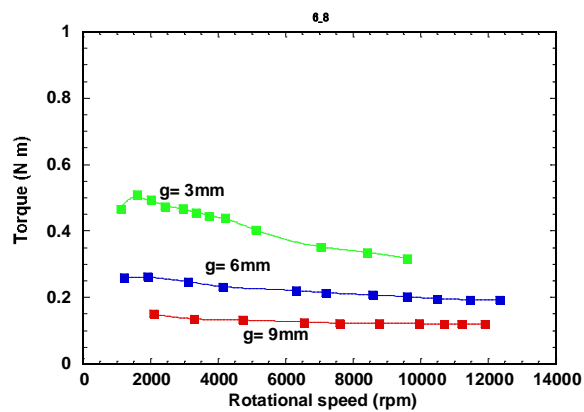


Fig.6 Torque required to rotate magnetic wheel.

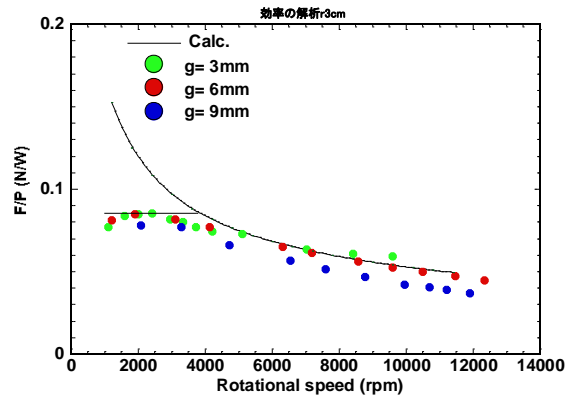


Fig.7 σ for rotational speed.

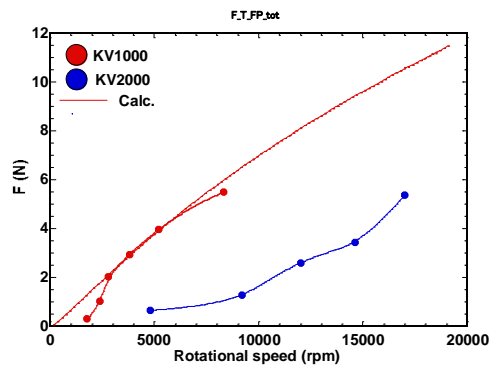


Fig.8 Measured levitation force using small magnetic wheel and Cu plate. KV1000:

low-speed motor, KV2000: high-speed motor

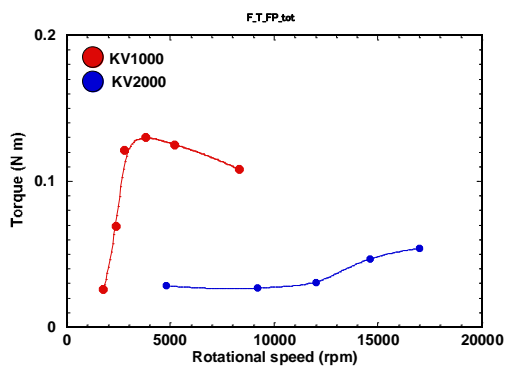


Fig.9 Torque required to rotate magnetic wheel.

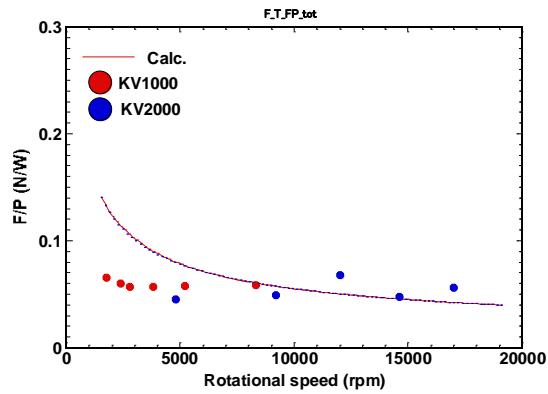
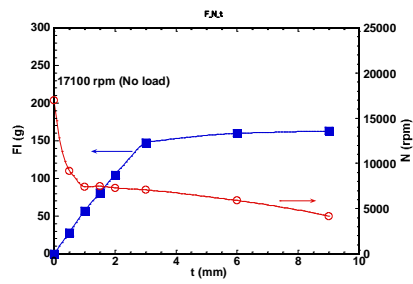
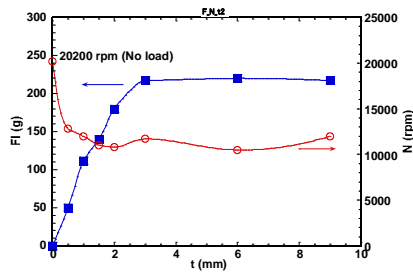


Fig.10 Levitation force per required power.

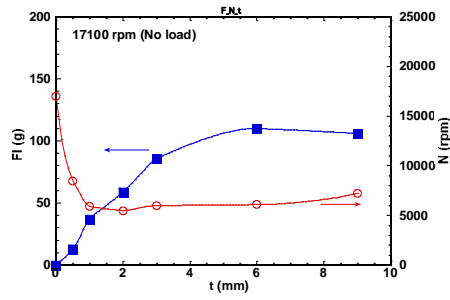


(a)

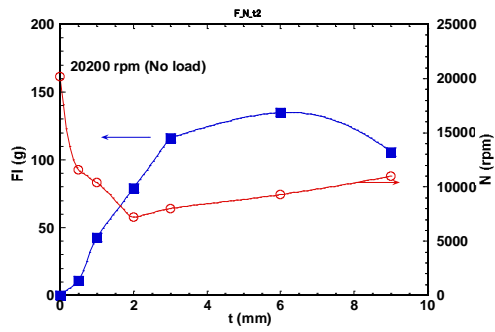


(b)

Fig.11 Measured floating force and rotation speed for magnetic wheel using Cu plate. (a) Rotation speed with no load was 17000rpm. (b) Rotation speed with no load was 20200rpm.

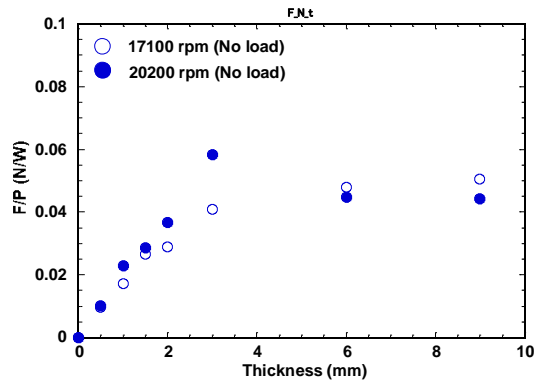


(a)

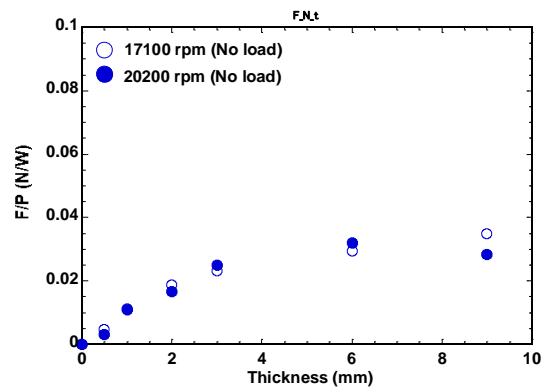


(b)

Fig.12 Measured floating force and rotation speed for magnetic wheel using Al plate, (a) rotation speed with no load was 17000 rpm, (b) rotation speed with no load was 20200 rpm.



(a)



(b)

Fig.13 F_L / P as a function of thickness. (a) Cu plate, (b) Al plate.

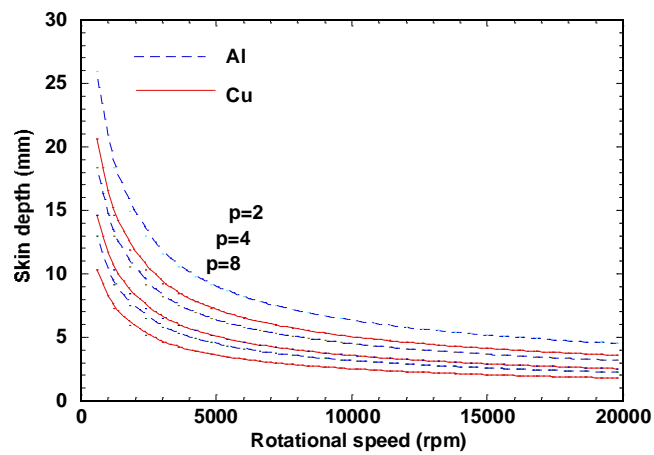


Fig.14 Calculated skin depth as a function of pole number. (A) Using Al plate, (B) Using Cu plate.

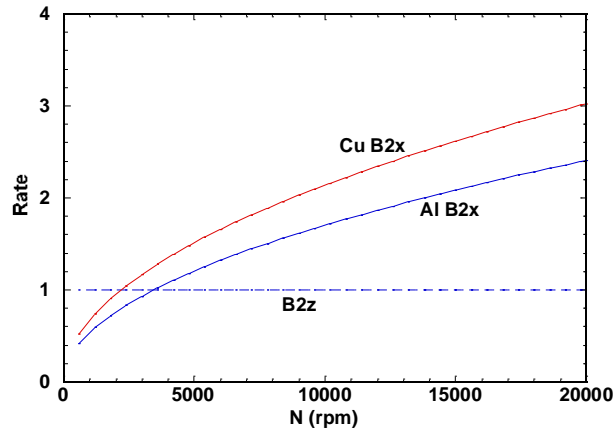
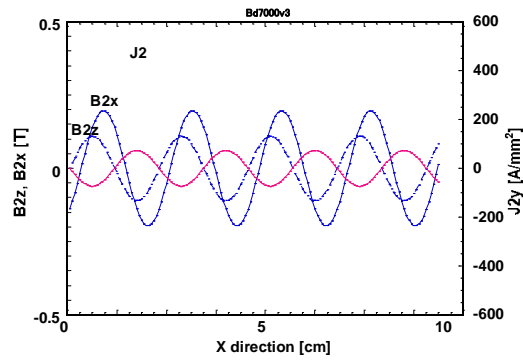
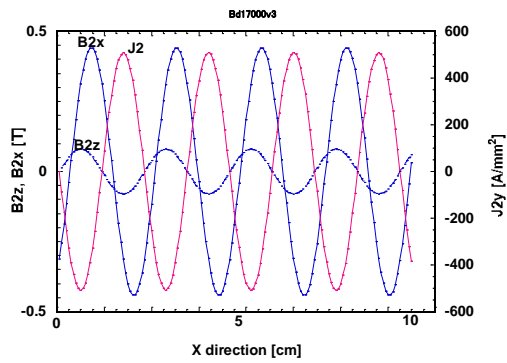


Fig.15 Calculated B2x for B2z.



(a)



(b)

Fig.16 Calculated B2x for B2z. J2y (a)7000rpm,(b)17000rpm. z=0cm.

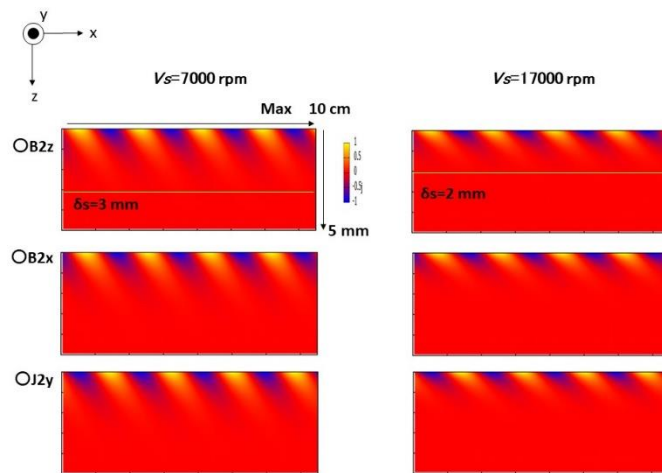
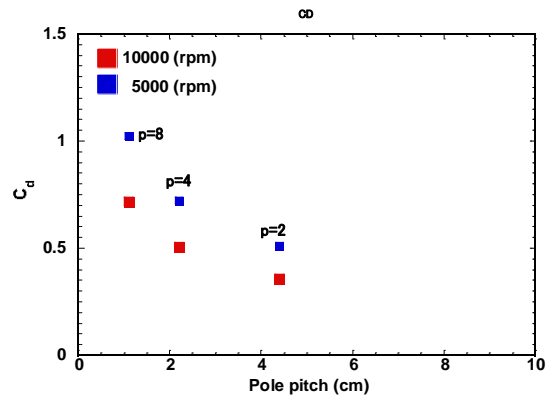
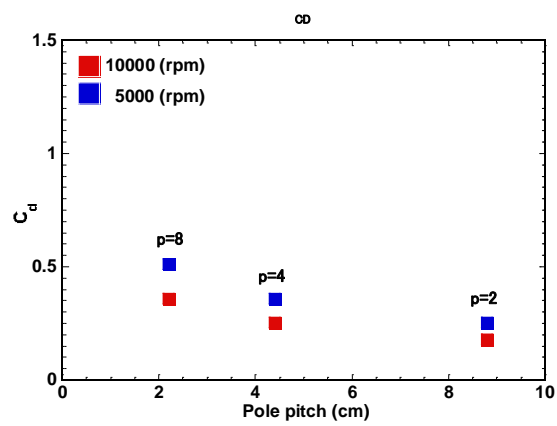


Fig.17 Calculated distribution of magnetic flux density and current density.



(a)



(b)

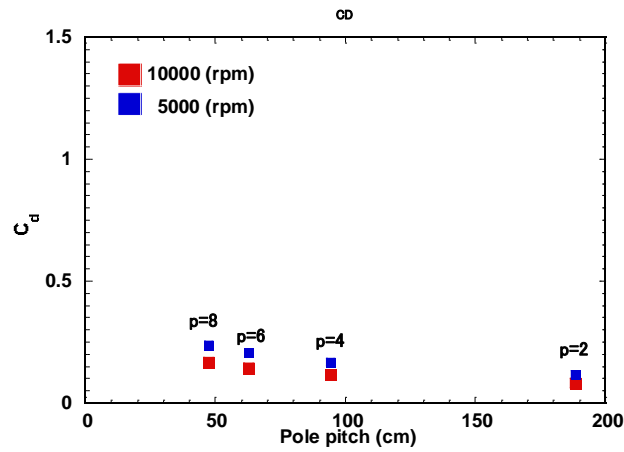
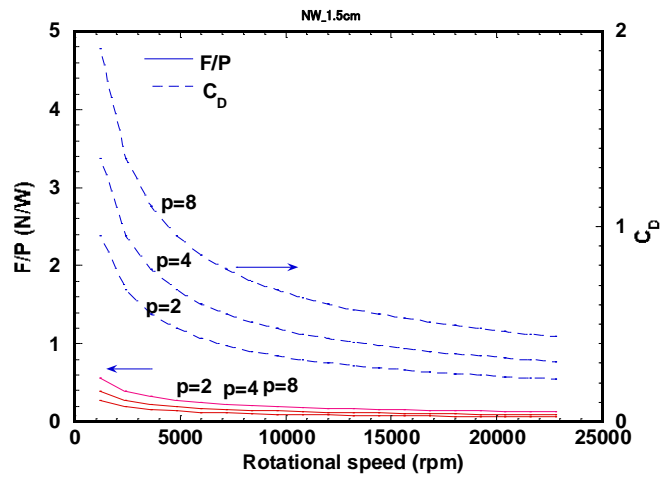
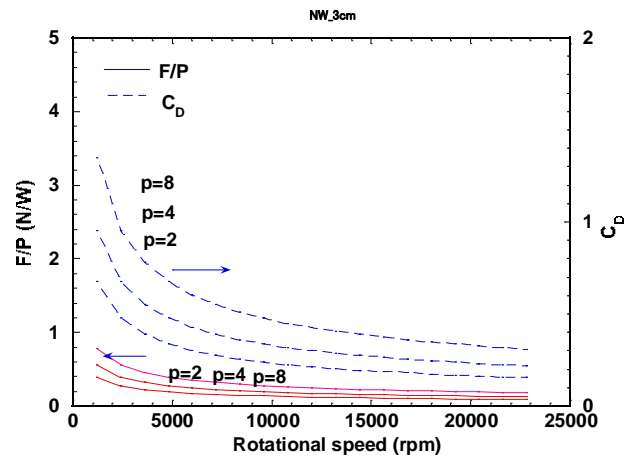


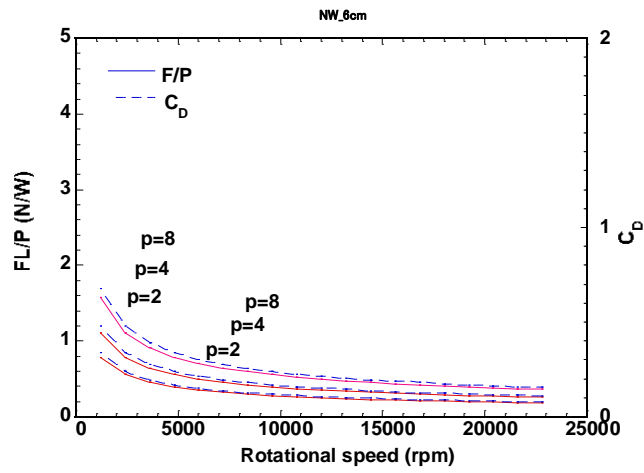
Fig. 18 Caclulated C_d using Cu plate as a function of pole pitch. (a) $r = 1.5\text{cm}$, (b) $r = 3.0\text{cm}$ (c) $r = 6.0\text{cm}$.



(a)



(b)



(c)

Fig. 19 Calculated C_d using Cu plate as a function of rotational speed. (a) $r = 1.5\text{cm}$,

(b) $r = 3.0\text{cm}$ (c) $r = 6.0\text{cm}$.

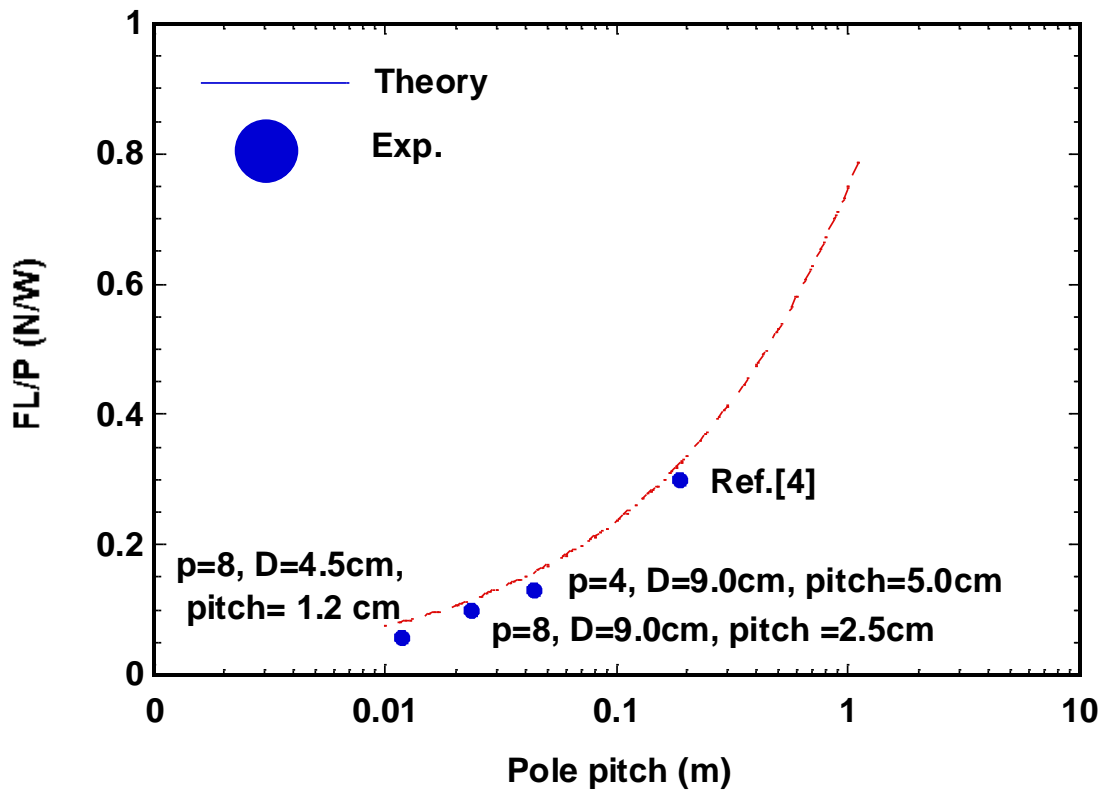


Fig.20 Calculated σ as a function of pole pitch and comparison with experimental results using Cu plate. Here, P was set to be the electrical output power of motor.